Advances in Biological Research 7 (6): 253-265, 2013
ISSN 1992-0067

DOI: 10.5829/idosi.abr.2013.7.6.76164

Spermatogenesis and Sperm Ultrastructure in the Land Slug *Limax flavus* (Gastropoda, Pulmonata) from Egypt

Irene Sameh Gamil

Department of Zoology and Entomology,
Faculty of Science, Helwan University, Cairo, Egypt

Abstract: Spermatogenesis and sperm ultrastructure are examined and described for the first time in the garden slug *Limax flavus* (Gastropoda, Pulmonata, Stylommatophora) in Egypt. Spermatogonia show round nuclei with patchy heterochromatin. The primary spermatocytes are characterized by the presence of synaptonemal complexes. The secondary spermatocytes are reduced in size and contain less cytoplasm and clustered stacks of Golgian cisternae with small proacrosomal vesicles lying close to them. During spermiogenesis, electron-dense plaques develop at both the future anterior and posterior poles of the nuclear surface. These plaques determine the apparent antero-posterior axis of the spermatid, the distal plaque indicates the future anterior part of the cell and the basal one the posterior part where an abundant number of mitochondria are aggregated. The mature spermatozoon shows the characteristic sperm features: an acrosomal vesicle supported by an acrosomal pedestal; a helically keeled nucleus, a neck region and a complex elongate middle piece featuring paracrystalline and matrix layers sheathing the axoneme, coarse fibers and glycogen helices.

Key words: Spermiogenesis · Spermatozoa · Hermaphrodite snail · Mollusca · Pulmonate

INTRODUCTION

The bulk of the land Gastropoda consists of Pulmonata including the most important order Stylommatophora which is one of the most diverse and economically significant groups of living molluscs [1]. *Limax flavus* (Linnaeus, 1758) (Pulmonata, Stylommatophora) is a medium to large species of air breathing land slug in the family Limacidae.

Ultrastructural features of spermatogenesis stages and spermatozoa in terrestrial gastropods have been described in some pulmonate species [2-13]. According to Healy [1], Spermatogenesis includes four developmental stages: derivation of spermatogonia from the germ cells, mitotic proliferation of spermatogonia, production of primary and secondary spermatocytes followed by the spermatids and their eventual transformation into mature spermatozoa.

The hermaphroditic nature of pulmonates necessitates differentiating between those spermatozoa produced by an individual (autospermatozoa) and those received by that animal during copulation (allospermatozoa or heterospermatozoa) [1]. In the present study, a detailed description of spermatogenesis process till the formation of mature autospermatozoa is presented. Studies on the spermatozoa and spermatogenesis have been used extensively to explore taxonomic and phylogenetic relationships of gastropods, as sperm morphology is most conservative and therefore of most taxonomic and phylogenetic value [1, 14-16]. The available comparative studies of stylommatophoran spermatozoa suggest that spermatozoon features may prove taxonomically and phylogenetically informative, as they have in other groups of gastropods [1].

On the other hand, terrestrial molluscs including snails and slugs are destructive agricultural pests causing economic damage to a wide variety of plants including horticulture, field crops and forestry; in addition, they are important in medical and veterinary practice [17]. Despite many studies on the biology of *L. flavus* [18], the ultrastructural description of the spermatogenesis was never reported. The aim of the present work is to study the general aspects of spermatogenesis in *L. flavus* and to describe for the first time the spermatozoon of this species.

Corresponding Author: Irene Sameh Gamil, Department of Zoology and Entomology,
Faculty of Science, Helwan University, Cairo, Egypt.

MATERIALS AND METHODS

Adult specimens of the land slug *Limax flavus* (Linnaeus, 1758) were collected from the nursery of ornamental plants at Giza Governorate during spring months of 2012 and treated for transmission electron microscopy. First they were euthanized by placing them in a culture dish and gently cover with carbonated water (club soda) and then they were dissected.

Small pieces of the ovotestis were fixed in 2% gluteraldehyde in 0.1M phosphate buffer, pH 7.3, for 2 h at 4°C. Following a buffer wash, tissues were postfixed in 1% osmium tetroxide in 0.1 M phosphate buffer at pH 7.3 for 1 h, ultrathin sections were cut using a diamond knife of an LKB 4800 Ultratome, mounted on uncoated copper grids and double stained with alcoholic uranyl acetate and aqueous lead citrate for 20 min. Ultrathin sections were viewed in a Joel 1200 EX2-transmission electron microscope at 80 kV.

RESULTS

The ovotestis of *L. flavus* is made up of a large number of oval or circular acini separated by connective tissues. Each acinus has a thin wall of germinal epithelium resting on a distinct basement membrane and encloses a wide lumen. Germ cells become differentiated from the germinal epithelium.

Spermatogonia arise from the germinal epithelium and become attached via desmosome-like junctions to Sertoli cells and form a cluster (Fig.1A, B). Sertoli cells are also differentiated from the germinal epithelium; they displayed a triangular shape with lysosomes. Spermatogonia are generally pyriform and exhibit an oblong to spherical nucleus with patchy heterochromatin and eccentrically located nucleoli, in addition to a relatively small cytoplasm containing round to oblong mitochondria. In some instances, two secondary spermatogonia develop within a common cytoplasm during spermatogonial proliferative divisions (Fig. 1C).

Spermatogonia divide producing the primary spermatocytes which are round to polygonal in shape, and characterized by an increased proportion of cytoplasm relative to the nuclear volume and, within the nucleus, the presence of synaptonemal complexes (Fig. 1D). Primary spermatocytes are usually found in groups and their nuclei are surrounded by nuclear wrinkles and packed with chromatin granules. They divide giving rise to the secondary spermatocytes which are reduced in size compared with the primary ones and contain proportionately less cytoplasm and clustered stacks of Golgian cisternae with small proacrosomal vesicles containing electron dense material lying close to them (Fig. 1E). The large wrinkled nuclei of secondary spermatocytes are packed densely with chromatin granules and large conspicuous nucleoli, in addition, the mitochondria are located in proximity to the basal side of the nucleus (Fig. 1E). Cytoplasmic bridges are also seen between these cells (Fig.1F).

In early spermatids, the round nucleus begins to diminish in size and gradually migrates to one side of the cytoplasm; close to the cell membrane, and the mitochondria, aggregate on the opposite side near the nuclear envelope (Fig. 2A). The cytoplasm contains an extensive endoplasmic reticulum, usually multiple stacks of Golgi cisternae, numerous round or elongate mitochondria exhibiting unmodified cristae (Fig. 2A, C). As development proceeds, electron-dense plaques develop at both the future anterior and posterior poles of the nuclear surface. The apical dense plaque is associated with an acrosome determining the axis of the nucleus at early stage of spermiogenesis (Fig. 2B, C). The posterior plaque is more electron-dense and thicker than the anterior one and associated with internally located dense chromatin (Fig. 2C). These plaques determine the apparent antero-posterior axis of the spermatid, the distal plaque indicates the future anterior part of the cell and the basal one the posterior part where an abundant number of mitochondria are accumulated in addition to Golgi complexes (Fig. 2B, C). The nucleus is gradually compressed and becomes cup-shaped through a depression of the posterior portion (Fig. 2D).

A centriole giving rise to an axoneme with "9+2" microtubular pattern becomes lodged in the invaginated base of the nucleus, initially defined by the posterior nuclear plaque (Fig. 2D-F). The posterior depression of the spermatid nucleus deepens more and more with the appearance of a centriolar pit (nuclear fossa) in the vicinity of which starts the axoneme of the flagellum emerging among the mitochondria (Fig. 3A-C). The acrosome attaches to the middle of the anterior nuclear plaque (Fig. 3C) and seen in late spermatid supported by an acrosomal pedestal (Fig. 3H).

Once the acrosomal and centriolar-axonemal complexes have established their relationship with the anterior and posterior poles of the nucleus, respectively, the nuclear contents begin their transformation from fine granules to filaments (Fig. 3A-E, G, H). This is followed by the cluster of small cytoplasmic mitochondria along the length of the developing axoneme beginning fusion, thereby heralding the first phase of middle piece formation (Fig. 3D-F).

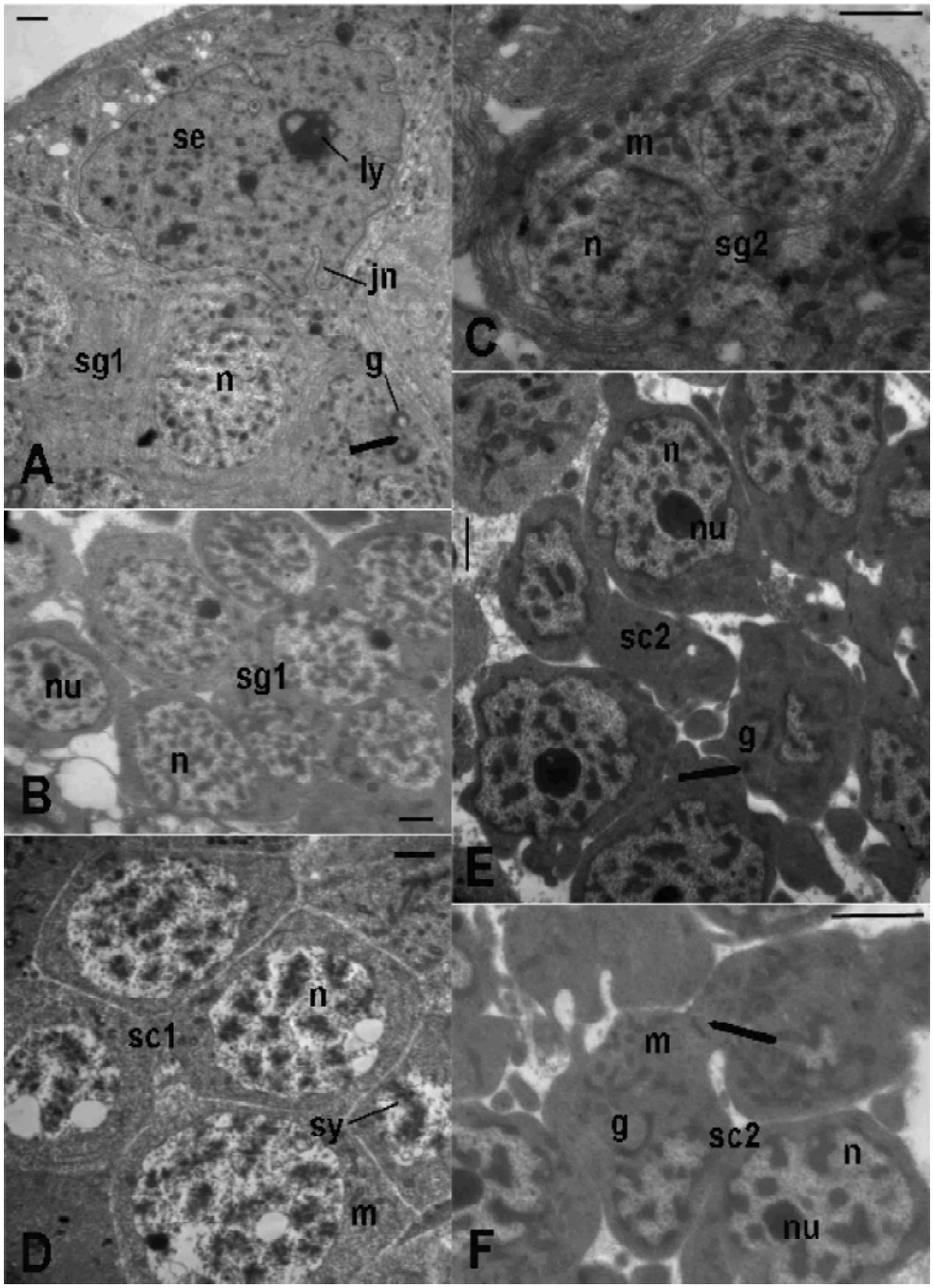

Fig. 1: Early stages of spermatogenesis of *Limax flavus*. **A.** A Sertoli cell with lysosomes and desmosome-like junctions, and surrounded by primary spermatogonia. Note the proacrosomal vesicles (arrow) in the vicinity of Golgi complexes. **B.** A cluster of primary spermatogonia with large nucleus and eccentric nucleolus. **C.** Two secondary spermatogonia within a common cytoplasm. **D.** A group of primary spermatocytes with wrinkled nuclear envelope. Synaptonemal complexes were observed. **E.** Secondary spermatocytes with wrinkled nuclear envelope, large nucleolus and dense chromatin granules. Note the proacrosomal vesicles (arrow) lying close to the Golgi complex. **F.** Secondary spermatocytes connected by a cytoplasmic bridge (arrow). Abbreviations: g, Golgi complex; jn, junction; ly, lysosomes; m, mitochondria; n, nucleus; nu, nucleolus; se, Sertoli cell; sg1, primary spermatogonia; sg2, secondary spermatogonia; sc1, primary spermatocyte; sc2, secondary spermatocyte; sy, synaptonemal complex. Scale bars: **A-F**= 2µm.

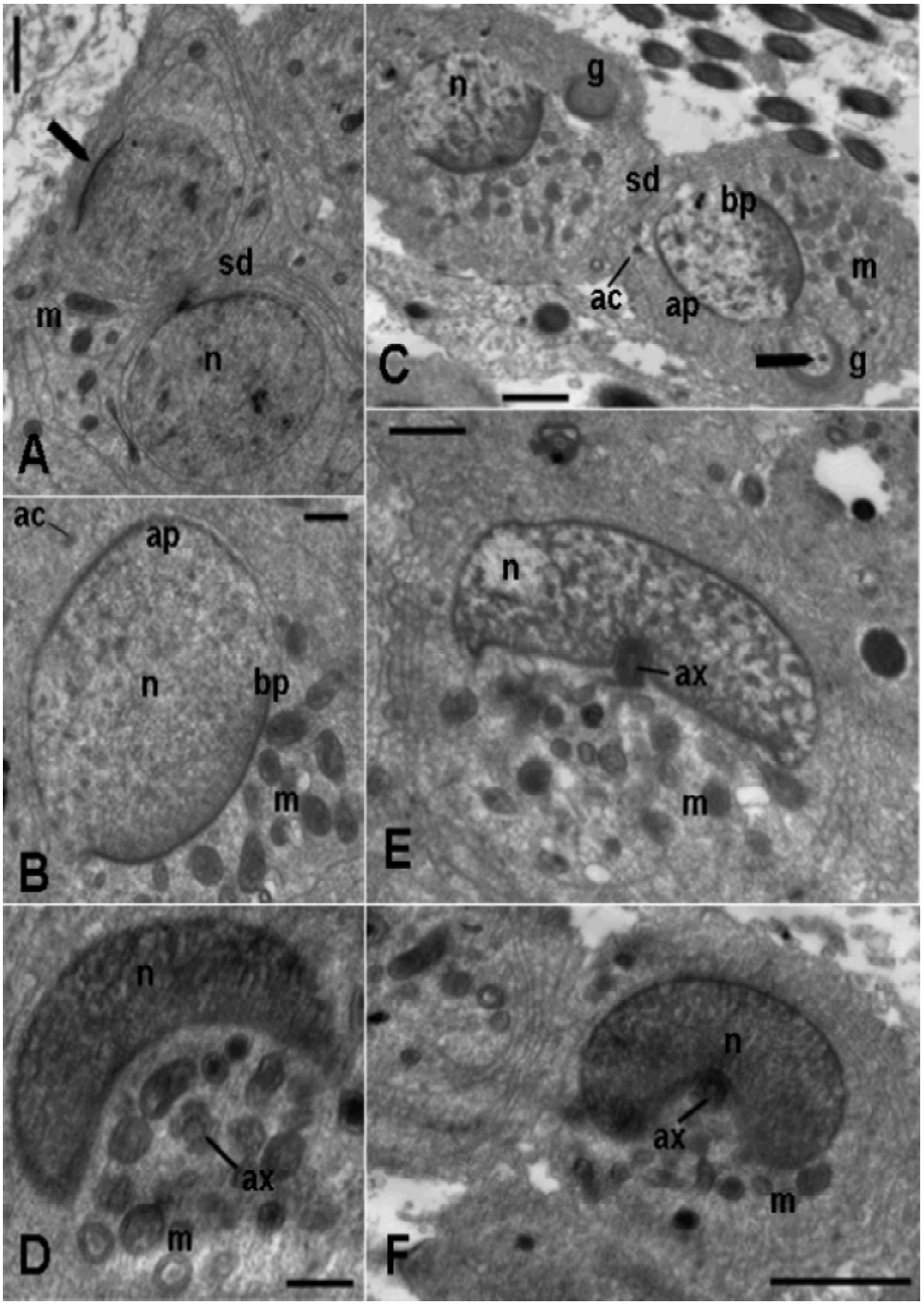

Fig. 2: Early spermatids of *Limax flavus*. **A.** Early spermatid with nuclear dense plaque (arrow). **B.** Nuclear apical and basal dense plaques in an early spermatid. The apical dense plaque is associated with an acrosome, while the mitochondria are grouped near the basal plaque. **C.** The nuclear basal plaque with more condensed chromatin, and accompanied externally with mitochondria. Nuclear polarization can be clearly seen. Note the proacrosomal vesicle lying close to the Golgi complex at the posterior pole of the cell. **D.** The spermatid nucleus becomes cup-shaped surrounding an axoneme and mitochondria. **E, F.** The spermatid nucleus takes on an axoneme and the mitochondria are still aggregated at the posterior pole. Abbreviations: ac, acrosome; ap, apical plaque; ax, axoneme; bp, basal plaque; g, Golgi complex; m, mitochondria; n, nucleus; sd, spermatid. Scale bars: **A**, **C, F**= 2µm, **B**, **D, E**= 500nm.

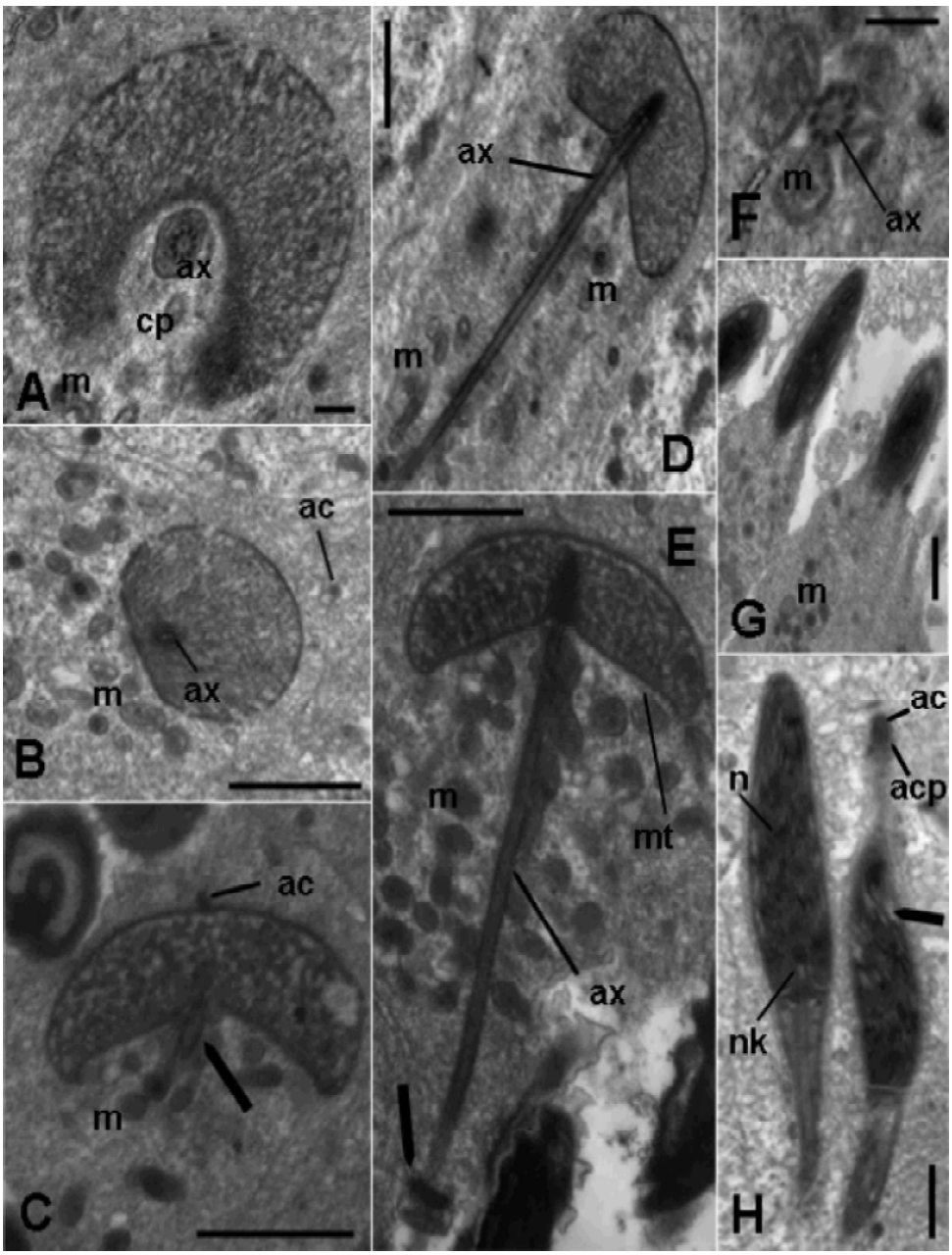

Fig. 3: Late spermatids of *Limax flavus*. **A.** The centriolar pit, formed by the cup-shaped spermatid nucleus, in the vicinity of which the axoneme develops. **B.** The spermatid nucleus encloses the axoneme. Note the aggregated mitochondria. **C.** Late spermatid nucleus with the axoneme growing and becoming perpendicular to the nucleus (arrow). Note the acrosome at the middle of the nucleus. **D.** Late spermatid with more developed axoneme. **E.** Late spermatid nucleus surrounded by microtubules. Note the mitochondrial incorporation within the spermatozoa around the axoneme. Note also the formation of glycogen helices (arrow). **F.** T.S. of the late spermatid showing the mitochondria surrounding the axoneme. **G.** Late spermatids with nuclear morphological changes. Note the mitochondria containing dense bodies and surrounded by membranes. **H.** L.S. of late spermatids with the acrosome, acrosomal pedestal, nucleus and neck region. The filaments of the spermatid nucleus are arranged parallel to each other and to the antero-posterior axis of the nucleus leaving clear spaces (arrow). Abbreviations: ac, acrosome; acp, acrosomal pedestal; ax, axoneme; cp, centriolar pit; m, mitochondria; mt, microtubules; n, nucleus; nk, neck region. Scale bars: **A, F**= 500nm, **B-E, G, H**= 2µm.

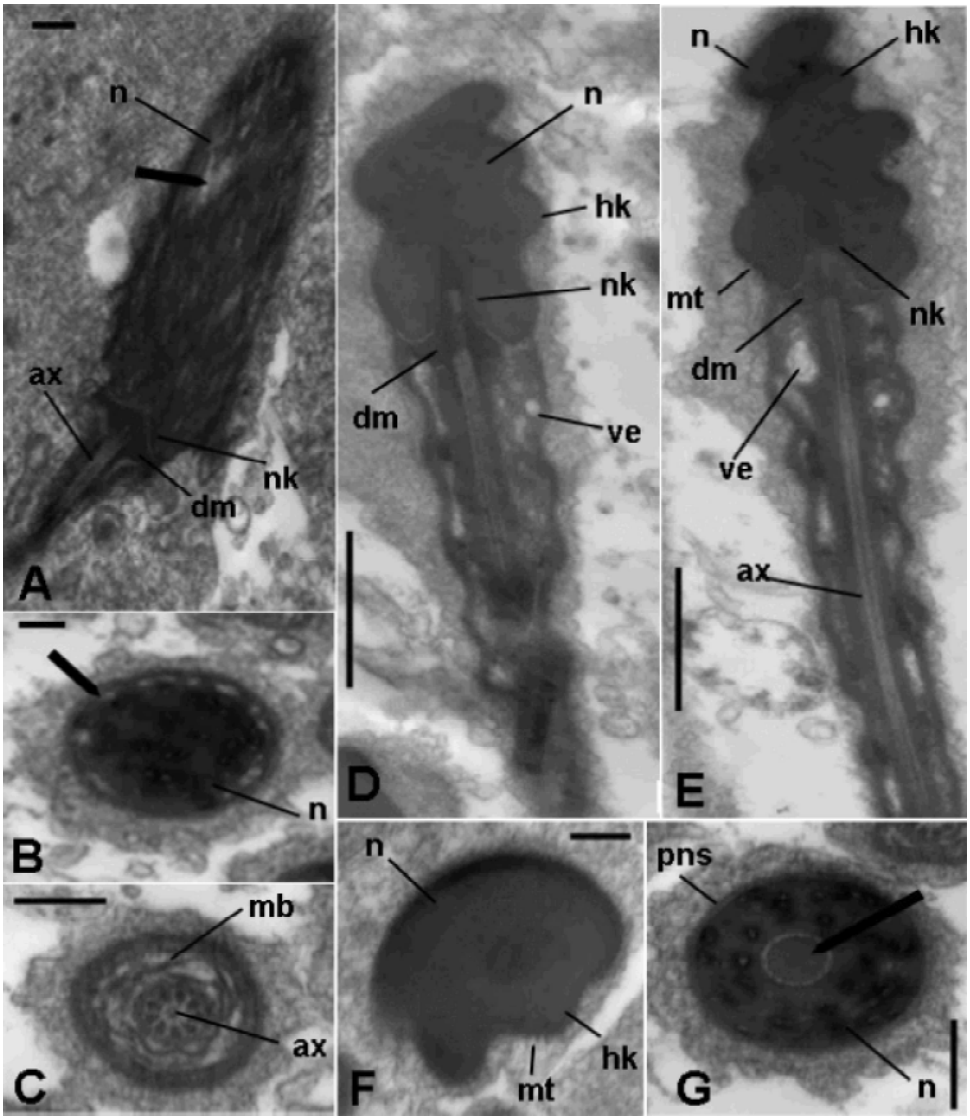

Fig. 4: Late spermatids and mature spermatozoa of *Limax flavus*. **A.** L.S. of a late spermatid showing the nucleus and neck region. Note the clear spaces between nuclear lamellae (arrow). Note also two expansions of dense material beneath the nucleus **B.** T.S. of a late spermatid showing the clear spaces (arrow) between nuclear lamellae. **C.** T.S. of a late spermatid showing membranes surrounding the axoneme. **D, E.** L.S. of spermatozoa with prominent nucleus and neck region. The nucleus is knobbed, with helical keels and surrounded by microtubules. Note the two expansions of dense material extending beneath the nucleus. Note also small vesicles within the cytoplasm. **F.** T.S. of the spermatozoon nucleus showing the helical keels and microtubules. **G.** T.S. of the spermatozoon nucleus at the most posterior part showing the centriolar pit (arrow), where the neck region is inserted. Note the perinuclear sheath surrounding the nucleus. Abbreviations: ax, axoneme; dm, dense material; hk, helical keel; mb, membranes; mt, microtubules; n, nucleus; nk, neck region; pns, perinuclear sheath; ve, vesicle. Scale bars: **A-C, F, G**= 500nm, **D, E**= 2µm.

The chromatin condensation into filaments increases more and more and these filaments become arranged parallel to the long axis of the nucleus, the basis of the nucleus remains wider than the apex (Fig. 4A). During further development, the nucleus of the late spermatids (or young spermatozoa) are lengthened, meanwhile, the lamellae thickened leaving only a few spaces between them (Figs 3H, 4A, B). Several membranes surround roughly the developing axoneme (Fig. 4C).

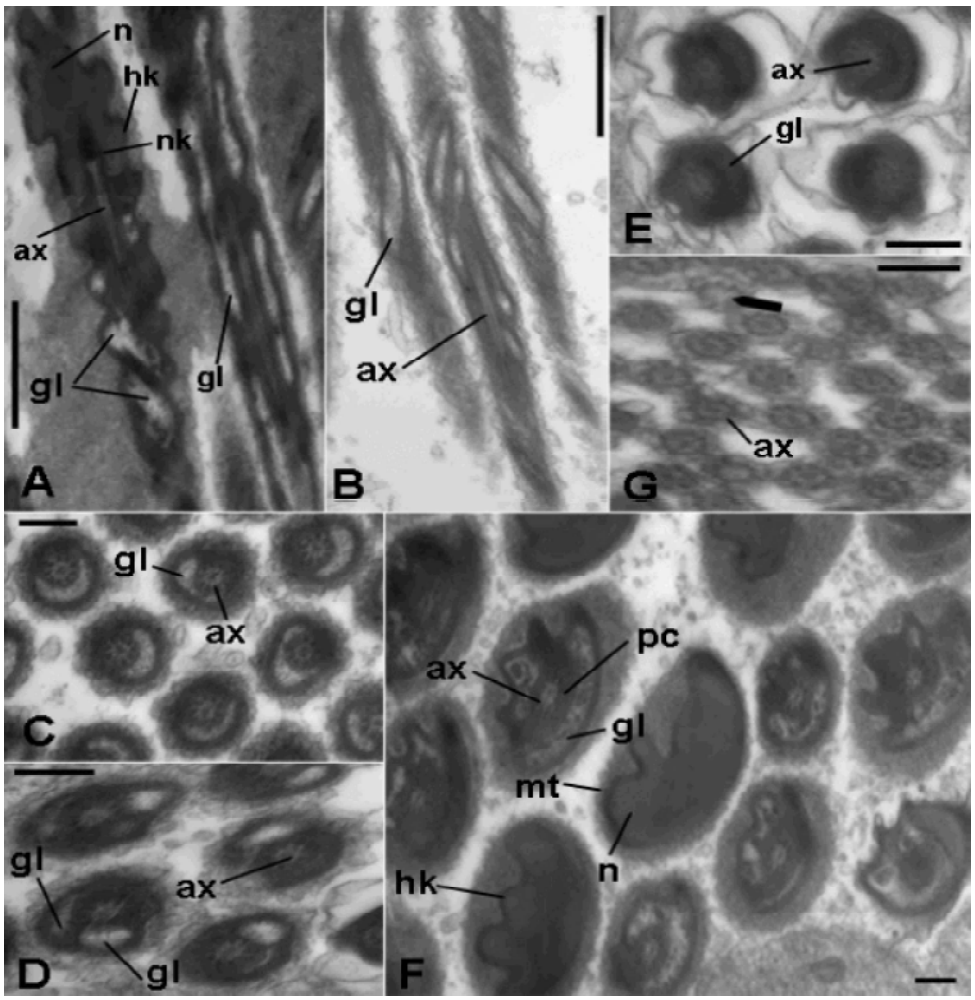

Fig. 5: Mature spermatozoa of *Limax flavus*. **A.** L.S. of mature spermatozoa with the nucleus, helical keels, neck region and the mitochondrial complex spiraling around the axoneme. Note the formation of glycogen helices. **B.** L.S. of mature spermatozoa showing two glycogen helices spiraling around the axoneme. **C.** T.S. of the spermatozoa showing the first glycogen helix around the axoneme. **D.** Two glycogen helices surrounding the axoneme. **E.** T.S. of the spermatozoa showing the third glycogen helix spiraling around the axoneme. **F.** T.S. of the spermatozoa showing the paracrystalline layer and matrix components of the mitochondrial derivative and the glycogen helix. Note the helical keels of the nucleus surrounded with microtubules. **G.** T.S. at the posterior end of the spermatozoa showing the absence of helical structures around the axoneme. Note the disappearance of the central element in some axonemes (arrow). Abbreviations: ax, axoneme; gl, glycogen; hk, helical keel; m, mitochondria; mt, microtubules; n, nucleus; nk, neck region; pc, paracrystalline layer. Scale bars: **A, B**= 2µm, **C-G**= 500nm.

The mature spermatozoon is very long and all parts are helically coiling around the long axis of the cell. It consists of three parts: the nucleus (the head region), the neck region (the midpiece) and the middle piece (the midpiece, the glycogen piece or the tail).

The Nucleus: The helically keeled and knobbed nucleus tapers anteriorly and the chromatin components are very condensed (Fig. 4D-G). The microtubules surround the nuclear envelope covering the whole length of the nucleus (Fig. 4E, F). Posteriorly, the nucleus has a deep V-shaped nuclear fossa (centriolar pit) which houses the electron-dense centriolar complex from which the course fibers of the axoneme emerge, so this posterior depression acts as a socket for the neck region (Fig. 4D, E, G). A perinuclear sheath formed of a homogeneous single layer of granular material encloses almost the whole nucleus (Fig. 4G).

The Neck Region: The neck region is the most posterior spiral of the nucleus showing the beginning of the axoneme of the flagellum; it fixes the middle piece to the head. An amorphous substance filled up the inner portion of the conical nuclear fossa in addition to two expansions of dense material extending beneath the nucleus (Fig. 4A, D, E). Dense material almost always obscures the micro-tubular structure of the axoneme where it penetrates the basal invagination of the nucleus.

The Middle Piece: The middle piece is the longest part of the mature spermatozoon. It is formed by the axoneme and the mitochondrial complex (as round mitochondria fuse in a continuous sheath around the axoneme and begin the first step of elongation and internal reorganization). The cytoplasm contains many small vesicles (Fig. 4D, E). During development of the middle piece, the mitochondrial material forms three helical channels (the glycogen helices) (Fig. 5A-E), in addition, an essential reorganization of the mitochondrial materials into discrete layers of matrix material occurs with highly structured arrangements of paracrystalline particles (Fig. 5F).

The helical channels run parallel to one another throughout most of the length of the spermatozoa; this begins with the formation of two helices containing electron dense granules in a clear substrate (Fig. 5A-D), followed by one helix containing an amorphous material (Fig. 5E). The last portion of the spermatozoon consists of the axoneme taking an approximately central position for the whole length of the tail. There is a progressive disorganization of the axoneme towards the posterior end and the central element disappears (Fig. 5G).

DISCUSSION

Spermatogenesis of *L. flavus* was found to occur in the classical manner. Basically, the steps leading to the spermatozoa formation follow the general developmental patterns of spermatogenesis and are similar to those described for various pulmonates [1, 12].

The close contact between spermatogonia and Sertoli cells has previously described in the ovotestis of the Neotropical *Scutalus tupacii* [10] and the terrestrial pulmonate *Helix aspersa* [19]. Desmosome-like junctions provide strong adhesive sites between Sertoli cells and germ cells in *Arion hortensis* [20]. Sertoli cells of *L. flavus* are provided with lysosomes; large phagolysosomes with degenerated germ cells were also recorded in the bibalve molluscs *Pitar rudis* and *Chamelea gallina* (Veneridae) [21]. Lysosomes and multivesicular bodies in the Sertoli cells of *S. tupacii* may be due to the destruction of the rest of the spermatid cytoplasm after spermination [10]. While, Zabala *et al.* [22] have concluded that Sertoli cells of the volutid *Adelomelon ancilla* have the capacity to phagocytose residual cytoplasm through the action of the residual bodies and myeloid bodies.

Spermatogonia and spermatocytes of *L. flavus* remain linked by intercellular bridges, as it was observed in other pulmonates [12] as well as many prosobranchs [23] where intercellular bridges persist until advanced stages of spermatogenesis. The wrinkled nuclei of spermatocytes of *L. flavus* were also noticed in *A. rufus* [12].

Healy [1] determined that in terrestrial gastropods, as in other internally fertilizing molluscs, the process of spermiogenesis involves the formation of the acrosome, condensation of the nuclear contents, completion of associated nuclear protein transitions, and formation of an elongate midpiece and finally, the deposition of whatever glycogen reserves around the mitochondria and/or axoneme; generally, these events overlap, although certain spermiogenic features such as the appearance of the cytoplasmic microtubular sheath occur only late in the process.

There is a thickening of the nuclear envelope covering the anterior and posterior surfaces of young spermatids nuclei of *L. flavus* forming the anterior and posterior plaques, respectively. Similar observations have been noted in the spermatids of other pulmonates [4, 12]. The polarity of the spermatid nucleus is probably already determined in early spermatocytes, by the accumulation of the cytoplasmic organelles on the side which will become the posterior part of the spermatozoon [12] as also examined in the spermatocytes of *L. flavus*.

Small proacrosomal vesicles are recorded in *L. flavus* lying close to the stacks of Golgi complex agreeing the conclusion of their synthesis from Golgi complex. Such observation was recorded in the pulmonate *S. tupacii* [10]. On the other hand, rough endoplasmic reticulum shares the Golgi complex in the synthesis of proacrosomal vesicles in *P. rudis* and *C. gallina* [21].

The shape of the acrosome as a cylindrical structure between the acrosomal vesicle and the nucleus is very similar among different species of pulmonates [6, 12]. The acrosomal complex of most investigated terrestrial pulmonates is situated at the nuclear apex; parallel to the spermatozoon longitudinal axis or slightly tilted in relation to it [4, 10, 11, 14, 24-26]. In *Onchidella celtica*, the principal body of the cylindrical acrosome structure is flanked by two electron-dense elliptical elements presenting a more complex structure [16]. While in *Cantareus asperses*, the acrosomal complex is reflected

backwards from the nuclear apex in the spermatozoa taken from the hermaphrodite duct and the spermatophores [7]. On the other hand, a typical acrosome cannot be seen in some stylommatophorans, instead a finely granular homogeneous material surrounds the apex of the nucleus [27], or a granulated material appears only on one side of the terminal spiral of the nucleus [5]. Nevertheless, the structure of the acrosome may be of phylogenetic value [28]. According to Medina *et al.* [29] the substructure of the acrosomal pedestal in *Hypselodoris tricolor* could provide the acrosome with greater resistance to frontal push in order to facilitate the entry into the egg during fertilization.

In Pulmonata, the Golgi complex secretes a round acrosomal vesicle which migrates to the center of the anterior nuclear plaque and becomes fixed there, and during the migration process, the acrosomal vesicle acquires a supporting cylinder [1] which is the case in *L. flavus* where proacrosomal vesicles were seen in the vicinity of Golgi complexes and the acrosome migrates until becomes attached to the middle of the anterior plaque determining the axis of the nucleus at early stage of spermiogenesis, such events were also previously described in *A. rufus* [12]. The secretion of proacrosomal vesicles from Golgi complexes has also described in some caenogastropods (Prosobranchia) [22]. On the other hand, the endoplasmic reticulum incorporates in the formation of the proacrosomal vesicles besides the Golgi complex in few species of Veneroidea [21].

Cuezzo [10] has recorded the formation of the implantation fossa in the secondary spermatocytes of *S. tupacii*, this structure was recorded in the spermatids of *A. rufus* [12] as in *L. flavus* as a centriolar pit or nuclear fossa. Such structure was previously defined as a centriolar adjunct-like in the neck region of midspermatids in the opisthobranch *Hypselodoris tricolor* [30].

Both the few spaces appearing among the nucleus lamellae, and the membranes surrounding the axoneme of the late spermatids (or young spermatozoa) in *L. flavus* were previously recorded in *A. rufus* [12]. Such membranes may play a supporting role in surrounding the newly developing axoneme especially as they disappear with spermatozoon maturation.

Azevedo and Corral [6] recorded no axonemal microtubules in the pulmonate *Siphonaria algestrae*, instead, nine homogeneous coarse fibers with transverse striations in the apical zone project toward the anterior section of the midpiece; these fibers are differentiated in a common microtubular axoneme in the posterior zone.

The spermatozoa of *L. flavus* belong to the "modified" type associated with internal fertilization as described by Franzén [31]. Spermatozoa of pulmonates like those of the rest of the hetero branch gastropods rank among the most complex in the animal kingdom [1] and show the same key features as: the presence of a round acrosomal vesicle associated with a columnar pedestal, a helical and/or helically keeled nucleus, an axoneme with "9+2" microtubular pattern associated with nine periodically striated coarse fibers and an extremely elongate and highly modified midpiece consisting of the axoneme, in addition to the mitochondrial derivative featuring matrix and paracrystalline arrays enclosing one or more glycogen-filled helical compartments (glycogen helices) [2, 5, 11, 12, 14, 15, 32]. Considering the spermatozoon length, Minoretti *et al.* [33] reported that stylommatophoran gastropods have extraordinarily long spermatozoa.

Generally, during the course of animal spermiogenesis, the cell nucleus undergoes a process of condensation, which depends upon specific proteins interaction with genetically controlled pattern of aggregation of DNA [34]. The nuclear chromatin is considered of little systematic value [13] as it takes different forms either fibrous [6, 16], or homogeneous [5, 7, 10, 24, 25].

Pulmonate spermatozoa nuclei show marked variation in the number and strength of the helical keels between taxa, as recorded by Healy [1] who added that in some groups, such as the Helicidae, the keels may appear almost vestigial. In most cases, the keels are dominant sculptural elements of the nucleus [2, 5, 11, 24]. Wilson and Healy [35] added that keels may enhance sperm movement. The lateral fin of the opisthobranchian Bullacta exarata spermatozoa may share the same function of Stylommatophora, and may also function in increasing the fertilizing efficiency [36].

In *L. flavus* the microtubules (the manchette as termed by Cuezzo [10] and Bergstrom and Arnold [37]) surround the nuclear envelope covering the whole length of the nucleus; this may offer the rigidity to the nucleus representing the head region of the mature spermatozoa. The microtubules are defined as the external force that supports and accompanies the nuclear transformation in *S. tupacii* [10]. In *A. rufus*, microtubules appear around the nucleus and are closely associated with the nuclear envelope and along the mitochondria derivate in a relation to the organization of the middle piece, especially in the late stages [12]. In addition, microtubules play some role

in forming the nuclear helical keels and the secondary helices within the midpiece sheath [1]. Zabala *et al*. [22] recorded that microtubules may be involved in the final twisting and shaping process of the nucleus and middle piece of *A. ancilla*, rather than making a role in their elongation. On the other hand, Hodgson and Bernard [38] had proposed that absence of a manchette in some patellid limpets suggests that the nuclear elongation is brought about from within the nucleus.

Martínez-Soler *et al*. [39] observed an absolute correlation between the perinuclear microtubules, the nuclear membrane and the chromatin fibers in the cephalopod *Sepia officinalis*; such observation was also noticed by Bergstrom and Arnold [37]. Martínez-Soler *et al*. [39] added that the perinuclear microtubule system does not only represent a structural element responsible for rigidity and shape of the spermatic nucleus, but also has a role in nucleocytoplasmic transport.

In *L. flavus*, a perinuclear sheath surrounds almost the whole nucleus and it seems to play an additional protection role. A number of stylommatophorans exhibits a perinuclear sheath associated with the acrosomal complex and the anterior portion of the nucleus [7, 11, 25]. This sheath is considered to be a unique feature among stylommatophoran sperms [1]. The perinuclear sheath may be either a single layer simply surrounding the nucleus [7] or formed of more than one layer [26] and may play a possible role in spermatozoa capacitation [40]. On the other hand, no perinuclear sheath was also reported in the pulmonate *Succinea putris* [41].

The subnuclear ring appearing where the mitochondrial derivative flares out to meet the nucleus in some chromodorid species (Opisthobranchia) [35], basommatophorans [13] as well as in some stylommatophorans [11] is not recorded in *L. flavus* in agreement with the conclusion of Giusti *et al*. [8] that this structure was assumed to be absent in stylommatophoran sperms.

In the neck region in *L. flavus*, a cone of amorphous material as well as two expansions of dense material exists around the anterior end of the axoneme; such structures were also noted in *A. rufus* [12]. In the middle piece, the mature spermatozoa possess a highly modified mitochondrial derivate composed of fused mitochondria that have undergone significant metamorphosis during spermiogenesis to form discrete paracrystalline and matrix layers. The function of these mitochondrial structural transformations is clarified by Cuezzo [10] as accurate indicators of the different spermatogenic stages. Three helically coiled glycogen channels are running parallel to one another throughout most of the length in *L. flavus* spermatozoa, and the axoneme is the only structure remaining in the posterior part of the tail piece. These structures have been described in many stylommatophoran pulmonates as well as opisthobranchs [5, 12, 14, 15, 24, 30].

Although the number of glycogen helices shows a great variation between taxa, almost all stylommatophoran spermatozoa exhibit only a single glycogen helix [1]. In *Limax* sp., Reger and Fitzgerald [42] recorded a single mitochondrion extending the entire length of the spermatozoon. Cuezzo [11] also recorded a single glycogen helix running along the middle piece in other pulmonates. However, three mitochondrial helices were recorded in the midpiece (middle piece) of the pulmonates *Anguispira alternate* [5] and *S. putris* [41], as well as in *A. rufus* as described by Pastisson and Lacorre [12] who noticed that in stylommatophoran molluscs, the glycogen helix is lacking in the tail complex. Up to four glycogen helices were reported in basommatophorans and some opisthobranchs [2, 24]. Giusti *et al*. [8] have noted that besides the constant large numbers of characters in Stylommatophora, the number of accessory helices in the midpiece is the only character suggesting an evolutionary trend from the lower to the higher stylommatophorans.

Glycogen granules are found within the tail piece of spermatozoa of all the fresh water and terrestrial pulmonates [12, 43] and can be synthesized within the glycogen helix of mature pulmonate spermatozoa through the activity of amylophosphorylase present in these cells [43]. Glycogen might be a substrate reserve for flagellar metabolism and an important source of glycolyzable material for the production of energy [44]; as well as it plays a significant role in maintaining long periods of spermatozoa viability [3, 14, 15, 32]. Although the accumulation of glycogen commences only after the completion of spermatozoa maturation, glycogen granules have been demonstrated in late spermatids and immature spermatozoa of certain basommatophorans [24]. Though, the structure of the middle piece may be of phylogenetic value [28].

The paracrystalline mitochondrial derivative is characteristic of both pulmonate and opisthobranch spermatozoa [3]. A paracrystalline complex is recorded between inner and outer mitochondrial membranes of *Limax* sp. [42].These mitochondrial structural transformations allow the use of these cytoplasmic organelles as accurate indicators of the different

spermatogenic stages [10]. Healy [1] concluded that the paracrystalline material consists of a three-dimensional, helically coiled, lattice-work composed of proteinaceous, hollow or granules.

Generally, the terminal portion of the sperm tail region of heterobranchs and basommatophorans shows a glycogen piece region preceded by an annulus (marking the junction between the midpiece and the glycogen piece) [13, 15, 35]; such structure appears to be uncertain or absent in previously studied stylommatophoran spermatozoa [7, 8, 10, 11, 25] as well as in *L. flavus*.

Healy [32] concluded that paraspermatozoa are completely absent in Opisthobranchia and Pulmonata. Healy [1] added that there is no firm evidence to support the occurrence of spermatozoon dimorphism in any species of Stylommatophora. Although marked spermatozoon dimorphism occurs widely in internally fertilizing prosobranchs.

It can be concluded that stylommatophoran spermatozoa are heterogeneous in morphology. They share many characteristics with other pulmonate spermatozoa, but differ from those of other gastropods, especially in their spermatozoon head and mitochondrial modifications.

REFERENCES

1. Healy, J.M., 2001. Spermatogenesis and oogenesis. In: The Biology of Terrestrial Molluscs, Ed., Barker, G.M. CABI Publishing, Wallingford, Oxon, pp: 357-382.
2. Thompson, T.E., 1973. Euthyneuran and other molluscan spermatozoa. *Malacologia*, 14: 167-206, addendum, pp: 443-444.
3. Anderson, W.A. and P. Personne, 1976. The molluscan spermatozoon: dynamic aspects of its structure and function. American Zoologist, 16: 293-313.
4. Parivar, K., 1981. Spermatogenesis and sperm dimorphism in land slug *Arion ater* L. (Pulmonata, Mollusca). Zeitschrift für Mikroskopische-Anatomie Forschungen, 95: 81-92.
5. Atkinson, J.W., 1982. An ultrastructural analysis of the mature spermatozoon of *Anguispira alternata* (say) (pulmonata, stylommatophora). Journal of Morphology, 173: 249-257.
6. Azevedo, C. and L. Corral, 1985. The fine structure of the spermatozoa of *Siphonaria algesirae* (Gastropoda, Pulmonata). Journal of Morphology, 186: 107-117.
7. Healy, J.M. and B.G.M. Jamieson, 1989. An ultrastructural study of spermatozoa of *Helix aspersa* and *Helix pomatia* (Gastropoda, Pulmonata). Journal of Molluscan Studies, 55: 389-404.
8. Giusti, F., G. Manganelli and G. Selmi, 1991. Spermatozoon fine structure in the phylogenetic study of the Helicoidea (Gastropoda, Pulmonata). Proceedings of the Tenth Malacological Congress, Tübinge, pp: 611-616.
9. Griffond, B., Z. Dadkhah-Teherant, A. Medina and M. Bride, 1991. Ultrastructure of *Helix aspersa* spermatogenesis: scanning and transmission electron microscopical contributions. Journal of Molluscan Studies, 57: 277-287.
10. Cuezzo, M.G., 1995. Spermatogenesis and sperm structure in the Neotropical pulmonate snail *Scutalus tupacii* (d'Orbigny). The Veliger, 38: 212-222.
11. Cuezzo, M.G., 2011. Ultrastructure of spermatozoa in Orthalicidae (Mollusca, Gastropoda, Stylommatophora) and its systematic implications. Zoomorphology, 130: 147-166.
12. Patisson, C. and I. Lacorre, 1996. Fine structure of the germinating cells during the spermiogenesis of *Arion rufus* (Mollusca, Pulmonate Gastropoda). Molecular Reproduction and Development, 43: 484-494.
13. Hodgson, A.N. and A.N. Healy, 1998. Comparative sperm morphology of the pulmonate limpets *Trimusculus costatus*, *T. reticulatus* (Trimusculidae) and *Burnupia stenochorias* and *Ancylus fluviatilis* (Ancylidae). Journal of Molluscan Studies, 64: 447-460.
14. Healy, J.M., 1988. Sperm morphology and its systematic importance in the Gastropoda. In: Prosobranch Phylogeny, Ed., Ponder, W.F. Malacological Review, Supplement, 4: 251-266.
15. Healy, J.M., 1996. Molluscan sperm ultrastructure correlation with taxonomic units within the Gastropoda, Cephalopoda and Bivalvia. In: Origin and Evolutionary Radiation of the Mollusca, Ed., Taylor, J.D. Oxford University Press, Oxford, pp: 99-113.
16. Selmi, M.G., F. Giusti and G. Manganelli, 1988. The fine structure of the mature spermatozoon of *Onchidella celtica* (Cuvier) (Mollusca: Gastropoda) and its phylogenetic implications. Journal of Ultrastructure and Molecular Structure Research, 99: 107-123.

17. Sallam, A. and N. El-Wakeil, 2012. Biological and ecological studies on land snails and their control. In: Integrated Pest Management and Pest Control-Current and Future Tactics, Eds. Larramendy, M.L. and S. Soloneski, pp: 414-444.
18. Azzam, K.M., 1999. Production of the snail parasitic nematode *Rhabditis* sp. from different pests. Proceedings of 1st Regional Symposium for Applied Biological Control in Mediterranean Countries Cairo, Egypt, pp: 25-29.
19. Griffond, B. and J. Bride, 1987. Germinal and non-germinal lines in the ovotestis of *Helix aspersa*: a survey. Roux's Archives of Developmental Biology, 196: 113-118.
20. Hou, S.T. and W.L. Maxwell, 1990. Desmosome-like junctions between sertoli-sertoli and sertoli-germ cells in the ovotestis of *Arion hortensis* (Mollusca: Pulmonata). Journal of Morphology, 205: 325-333.
21. Erkan, M. and M. Sousa, 2002. Fine structural study of the spermatogenic cycle in *Pitar rudis* and *Chamelea gallina* (Mollusca, Bivalvia, Veneridae). Tissue & Cell, 34: 262-272.
22. Zabala, S., G.N. Hermida and J. Giménez, 2012. Spermatogenesis in the marine snail *Adelomelon ancilla* (Volutidae) from Patagonia. Journal of Molluscan Studies, 78: 52-65.
23. Amor, M.J. and M. Durfort, 1990. Changes in nuclear structure during eupyrene spermatogenesis in *Murex brandaris*. Molecular Reproduction and Development, 25: 348-356.
24. Healy, J.M., 1983. An ultrastructural study of basommatophoran spermatozoa (Mollusca, Gastropoda). Zoologica Scripta, 12: 57-66.
25. Cuezzo, M.G., 1995. Ultrastructure of the mature spermatozoa of the land snail *Epiphragmophora tucumanensis* (Doering, 1874) (Gastropoda: Helicoidea). Journal of Molluscan Studies, 61: 1-7.
26. Bojat, N.C., U. Sauder and M. Haase, 2001. The spermathecal epithelium, sperm and their interactions in the hermaphroditic land snail *Arianta arbustorum* (Pulmonata, Stylommatophora). Zoomorphology, 120: 149-157.
27. Takaichi, S. and J.C. Dan, 1977. Spermiogenesis in the pulmonate snail, *Euhadra hickonis* 1. Acrosome formation. Development, Growth & Differentiation, 19: 1-14.
28. Hodgson, A.N., K.J. Eckelbarger and C.M. Young, 2009. Sperm ultrastructure and spermatogenesis in the hydrothermal vent gastropod *Rhynchopelta concentriaca* (Peltospiridae). Journal of Molluscan Studies, 75: 159-165.
29. Medina, A., J. Moreno and J.L. López-Campos, 1985. Acrosome evolution in *Hypselodoris tricolor* (Gastropoda: Nudibranchia). Journal of Submicroscopic Cytology, 17: 403-411.
30. Medina, A., J. Moreno and G. García-Herdugo, 1988. Sperm tail differentiation in the nudibranch mollusc *Hypselodoris tricolor* (Gastropoda, Opisthobranchia). Gamete Research, 20: 223-232.
31. Frazén, A., 1970. Phylogenetic aspects of the morphology of spermatozoa and spermiogenesis. In: Comparative Spermatology, Ed., Baccetti, B. New York, Academic Press, pp: 29-46.
32. Healy, J.M., 1987. Spermatozoan ultrastructure and its bearing on gastropod classification and evolution. *Australian Zoologist*, 24: 108-113.
33. Minoretti, N., P. Stoll and B. Baur, 2013. Heritability of sperm length and adult shell size in the land snail *Arianta arbustorum* (Linnaeus, 1758). Journal of Molluscan Studies, 79: 218-224.
34. Fawcett, D.W., W.A. Anderson and D.M. Phillips, 1971. Morphogenetics factors influencing the shape of the sperm head. Developmental Biology, 26: 220-251.
35. Wilson, N.G. and J.M. Healy, 2002. Comparative sperm ultrastructure in five genera of the nudibranch family Chromodorididae (Gastropoda: Opisthobranchia). Journal of Molluscan Studies, 68: 133-145.
36. Ying, X.P., W.X. Yang, N.C. Jiang and Y.P. Zhang, 2004. Ultrastructure of spermatozoa of *Bullacta exarata* (philippi) and its significance on reproductive evolution and physio-ecological adaptation. Journal of Zhejiang University SCIENCE, 5: 1211-1217.
37. Bergstrom, B.H. and J.M. Arnold, 1974. Nonkinetochore association of chromatin and microtubules. A preliminary note. The Journal of Cell Biology, 62: 917-920.
38. Hodgson, A.N. and R.T.F. Bernard, 1988. A comparison of the structure of the spermatozoa and spermatogenesis of 16 species of patellid limpet (Mollusca: Gastropoda: Archaeogastropoda). Journal of Morphology, 195: 205-223.
39. Martínez-Soler, F., K. Kurtz, and M. Chiva, 2007. Sperm nucleomorphogenesis in the cephalopod *Sepia officinalis*. Tissue cell, 39: 99-108.
40. Selmi, M.G., E. Bigliardi and F. Giusti, 1989. Morphological modifications in stored heterospermatozoa of *Oxyloma elegans* (Pulmonata: Stylommatophora). Journal of Ultrastructure and Molecular Structure Research, 102: 82-86.

41. Shilenko, L.V. and L.V. Danilova, 1979. Ultrastructure of the spermatozoids of the pulmonate molluscs, *Trichia hispida* and *Succinea putris*. Ontogenez, 10: 437-447.
42. Reger, J.F. and M.E. Fitzgerald, 1982. Studies on the fine structure of the mitochondrial derivative in spermatozoa of a gastropod. Tissue Cell, 14: 775-783.
43. Anderson, W.A. and P. Personne, 1970. The localization of glycogen in the spermatozoa of various invertebrate and vertebrate species. Journal of Cell Biology, 44: 29-51.
44. Maxwell, W.L., 1980. Distribution of glycogen deposits in two euthyneuran sperm tails. International Journal of Invertebrate Reproduction, 2: 245-249.